Supporting Information for:
Swelling and evaporation determine surface morphology of grafted hydrogel thin films

Caroline Kopecz-Muller[1,2,3], Clémence Gaunand[1,2], Yvette Tran[4,5], Matthieu Labousse[1], Elie Raphaël[1], Thomas Salez[3], Finn Box[1,2,6], and Joshua D. McGraw[1,2*]
[1] *Gulliver, CNRS, ESPCI Paris, Université PSL, 75005 Paris, France*
[2] *Institut Pierre Gilles de Gennes (IPGG), ESPCI Paris, Université PSL, 75005 Paris, France*
[3] *LOMA, CNRS, Univ. Bordeaux, F-33405 Talence, France*
[4] *Sciences et Ingénierie de la Matière Molle, CNRS, ESPCI Paris, Université PSL, 75005 Paris, France*
[5] *Sorbonne-Universités, UPMC Université Paris 06, 75005 Paris, France and*
[6] *Physics of Fluids & Soft Matter, Department of Physics & Astronomy, University of Manchester, Manchester M13 9PL, United Kingdom*

Number of pages: 7
Number of figures: 8

CONTENTS

* finn.box@manchester.ac.uk, joshua.mcgraw@espci.fr

S1. EXPERIMENTAL PROTOCOLS

A. Substrate preparation

The hydrogel samples studied here were made on either silicon wafers or thin glass substrates. The chosen substrates are cleaned in a freshly prepared "piranha" solution. 600 mL of this solution is prepared by mixing 200 mL of sulfuric acid (95-97%) and 400 mL of hydrogen peroxide (35%). The resulting solution was left to rest at room temperature for approximately 30 min, until it became a clear solution with no bubbles. The substrates were then immersed in this "piranha" solution for 1 h thoroughly, rinsed with deionized water, dried under pressurized nitrogen flow, rinsed with absolute ethanol, and finally dried again. Freshly cleaned substrates were chemically modified by grafting thiol groups on their surface in order to allow the hydrogel to attach to the substrate. 200 mL of silane solution was prepared by mixing 196 mL of absolute ethanol and 4 mL of 3-mercaptopropyltrimethoxysilane; this solution was left to rest for 1 h. Silanization was performed by immersing the substrates in this solution for 1 h. The substrates were then rinsed with absolute ethanol, and dried under nitrogen flow. All substrate preparation steps were done in a clean-room environment.

B. Hydrogel film preparation

The PNIPAM hydrogel used here [**?**] was prepared from a PNIPAM polymer that has been functionalized with ene-reactive groups, its molar mass is 459 kg/mol. The ene-functionnalized polymer solution was prepared by dissolving the copolymer in a 50/50 mixture of methanol and butanol, at the desired concentration (between 0.5 and 10 wt%). The solution was then left to rest overnight in the fridge. Just before use, dithioerythritol was added as a crosslinker: the quantity added was typically 60 wt% of that of the copolymer dissolved in solution. The solution was left to rest and homogenize for 20 min. The prepared solution was coated on the surface of thiolated substrates by spin-coating, with a spinning time of 30 s and different angular velocities in the range 500 to 4000 rpm (in the case of glass substrates, the solution was filtered with a 0.2 μm calibrated filter prior to spin coating). To remove excess solvent, the resulting polymer films were soft baked at 65°C for 1 min or dried under ambient conditions. Finally, the hydrogel was cross-linked by performing a UV-irradiation (λ_{UV}=254 nm) on the samples, with a fluorescent lamp for 0 min to 3 h (*n.b.* all measurements reported in the main text were performed on samples subject to 3 h of UV-irraditation). To remove uncured polymer and crosslinker excess, the resulting samples were either washed only with isopropanol HPLC grade, or first by immersion in deionized water for 4 h, then in isopropanol HPLC grade for 15 min. Finally, they were dried under ambient conditions.

C. Influence of polymer concentration and spin-coating speed on the film thickness

Sample thickness was modified by changing either the spin-coating speed or the PNIPAM solution concentration in the initial polymer solution (to modify its viscosity). This last parameter has the greatest influence: as shown in Fig. S1, modifying the PNIPAM concentration from 0.5 to 15 wt% allows the film thickness to be varied over almost three orders of magnitude (from $\sim$ 10 nm to 8 μm), for a given angular velocity of spin coating.

D. Influence of UV-exposure time and substrate type on ultrathin samples

Ultrathin samples, with thicknesses smaller than 70 nm, did not show any surface patterning either before or after the rinse step (see main text, Fig. 4). Additionally, since the surfaces remained flat, zero dependence on the substrate type or the evaporation rate of the spin-coating solvent was recorded. Ultrathin samples did, however, enable investigation of the influence of UV-exposure time on cross-linking of PNIPAM and the final thickness of the hydrogel films, as we now describe.

Ultrathin hydrogel samples were prepared from a 1% PNIPAM solution, as previously described, spin-coated at 3000 rpm. The samples were subjected to different UV-irradiation times (exposition carried out using a UV lamp, power 8 W, wavelength λ_{UV}=254 nm) and two evaporation methods after spin-coating, that lead to two evaporation rates: soft-baking (2 min at 65°C) or drying under ambient conditions (RT drying). These samples were prepared on two different types of substrate: functionalized silicon wafers and functionalized glass slides. In these particular experiments, samples were only rinsed

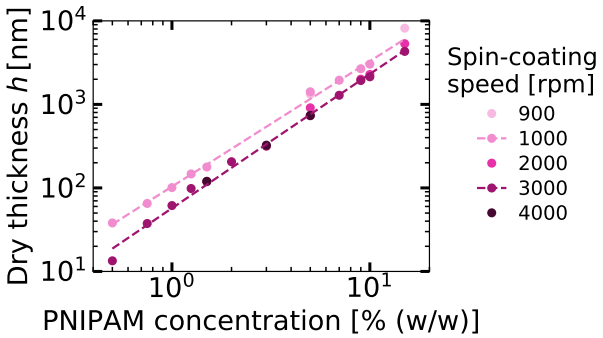

FIG. S1: **Dry thickness of the PNIPAM films as a function of PNIPAM concentration** *Sample thickness in the dry state h after rinsing as a function of PNIPAM solution concentration (wt%), for different spin-coating speeds as indicated by the legend.*

with isopropanol. They were observed before and after rinse and their thickness was measured, using atomic force microscopy (AFM). When samples were not irradiated with UV (*i.e.* zero irradiance time) no hydrogel was observed; the crosslinking network was unable to form, prohibiting the formation of a substrate-attached hydrogel.

Fig. S2 shows the time evolution of the thickness of samples grafted onto silicon wafers that underwent a soft-baking process and were exposed to UV irradiation for different periods of time, before and after rinsing. All the samples studied here were prepared with a 1 wt% PNIPAM solution and were spin-coated at 3000 rpm. We observe that 35 % to 50 % of the sample thickness to be removed during the rinse step. We believe that rinsing removes excess cross-linker and small polymer chains that are not attached to the polymeric network, since the high amount of removed matter is consistent with the proportional excess of cross-linker (nearly 38 wt%). UV-irradiation cures the polymer network – decreasing the amount of free unreacted cross-linker and small unattached chains – accordingly, we see that when UV-exposure time increases, the thickness of the removed portion tends to decrease. Additionally, we observed that the thickness of rinsed samples reaches a plateau at an exposure time of 1h30, suggesting that the cross-linking density would be homogeneous along the depth of the film in the plateau regime. Finally, these results are consistent with previous works, that establish the fabrication protocol of these type of samples and conducted their characterization [**?** **?**].

The results presented in this article were systematically obtained on samples that were exposed to UV for 3h and rinsed. We thus believe that the observed surface patterns do not result from any cross-linking gradient along the thickness of our PNIPAM films, in contrast to the observations of other works [**?**]. However, additional types of experiments such as small-angle spectroscopy could be performed to confirm the latter hypothesis. To understand what is the origin of the pattern formation, in the next section we exhibit AFM images of PNIPAM films at different stages of the fabrication process.

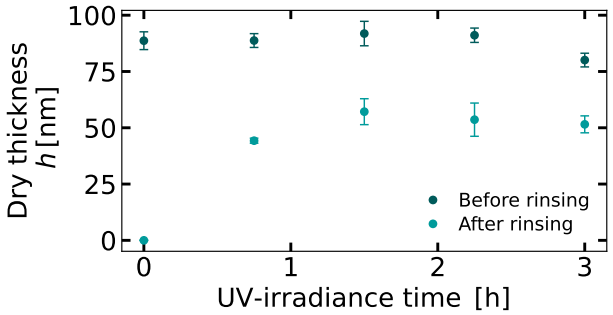

FIG. S2: **Influence of UV-exposure time and rinsing on sample thickness.** *Sample thickness in the dry state h as a function of the UV-irradiance time, before and after rinsing. The samples were prepared using a 1 wt% PNIPAM solution and spin-coating velocity of 3000 rpm. The values are averaged on 4 measurements.*

S2. EMPIRICAL ORIGIN OF PATTERNS

A. Determinant step for the formation of patterns

Sequential surface examination on dry samples during preparation enables identification of the preparation stage at which patterns appear. In Fig. S3, we show AFM images of two PNIPAM films, at different key steps of the fabrication protocol: right after spin-coating and evaporation of the solvent, after UV irradiance, after rinsing in water and drying, and after rinsing in isopropanol and drying. For thinner films (see Fig. S3, first row), no pattern appears. For sufficiently thick samples (see Fig. S3, second row), a surface pattern appears following the first rinsing-and-drying cycle, suggesting that the surface instability results from the swelling-deswelling process of the film. Finally, the subsequent swelling-and-drying cycle does not affect the formed pattern, suggesting that the deformation cycle is irreversible. In summary, the pattern is formed and fixed during the first rinsing-and-drying cycle.

B. Influence of the solvent evaporation rate and solvent type on thick samples

The creasing instability appears following immersion and rinsing of the cross-linked hydrogel film in a solvent, as showed in Fig. S3. This confirms that the surface patterning initially appears as a consequence of volumetric change, associated with imbibition-induced swelling, of the grafted, laterally-confined hydrogel. To study the influence of the (re)swelling of hydrogels in successive solvents, fully rinsed hydrogels that exhibited a pattern were immersed in two different, subsequent solvents – water and acetone – after preparation. The samples were then dried under two different conditions; using a nitrogen gun (which encourages a fast evaporation) and under ambient conditions (which results in a slower evaporation). Examples of sequential swelling and drying cycles are shown in Figs S4A and B, while the table shown in Fig. S4C indicates the samples preparation protocols. The surface patterning in a particular region-of-interest was observed on each sample before and after this secondary immersion and drying cycle, and the patterns were compared. For almost all samples, the exact same pattern can be recovered, showing that subsequent immersion and drying cycles had a negligible affect on the initial pattern features; an example is shown in Figs. S4 A and B. For two samples only, a slight amplitude decrease was observed, but is not considered to be a systematic effect of the experiment.

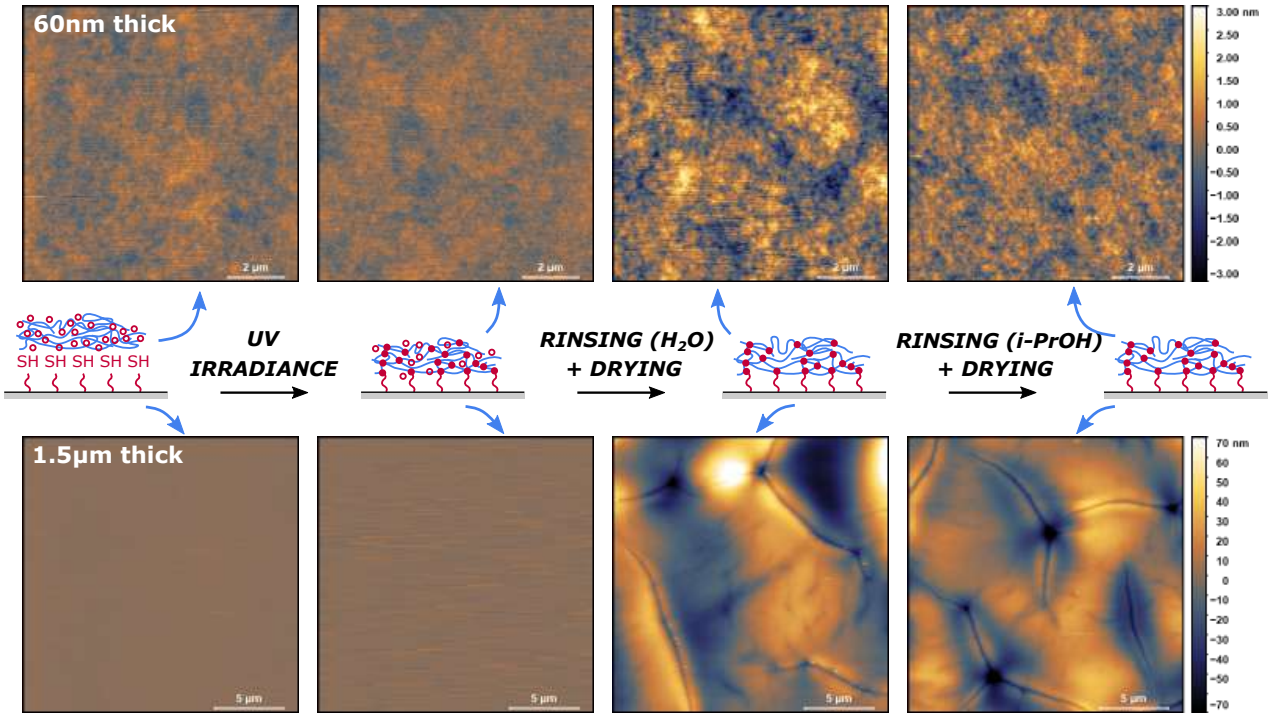

FIG. S3: **Topography of PNIPAM films during the fabrication process.** *AFM images of two dry PNIPAM films, at different steps of the fabrication process : after spin coating, after UV-irradiance, after a first rinsing-and-drying cycle in water and after a second one in isopropanol. Top row :* 60 nm *thick sample, fabricated using a spin-coating velocity of 3000 rpm and a PNIPAM solution concentration of 1 wt%. Bottom row :* 1.5 μm *thick sample, fabricated using a spin-coating velocity of 3000 rpm and a PNIPAM solution concentration of 9 wt%.*

This experiment shows that irrespective of the patterns shape and amplitude, they seem to be fixed and irreversible once they initially formed (*i.e.* during the first swelling and drying process). Our evidence suggests that the evaporation rate and its quality (related to its nature and to what extent it can swell the network) of any subsequent solvents seen by the hydrogel do not influence the surface pattern, contrary to what was evidenced in [**?**]. Instead, in our experiments, the first solvent seen by the system (*i.e.* water, during the first rinse step) that sets and fixes the pattern, induced network swelling and drying-induced shrinking.

To investigate the influence of evaporation rate of the first solvent on the surface patterning, hydrogels with patterns were prepared and rinsed only in water, with two different evaporation rates: a slow one, allowed by drying under ambient conditions, and a very slow one, achieved by drying in a covered beaker containing a water reservoir, with a small opening in the lid. In the first case, the sample dried in ~ 30 min; in the second case, drying took a few days. The surface topography of both samples was then measured by AFM. In Fig. S5A and B, we respectively show AFM images of the sample dried in 30 min and of the one dried in a few days. Both samples exhibit similar transition patterns when fully dried, as expected when considering their measured initial thickness of 2.02 μm. Additionally, we measure similar wavelengths of $\lambda \approx 30\,\mu$m and similar amplitudes of $A \approx 200$ nm on both samples. On the basis of this observation, we conclude that, for evaporation on the time scale of minutes to days, the evaporation rate has no influence on the pattern formation at the surface of our samples.

C. Additional AFM images of volcano patterns

The observation of volcano patterns at the surface of polymer films in the dry state is reproducible, for samples with dry thickness approximately equal to or above the critical threshold $h_c = l_{ec}^{wet}/S_R \approx 2\,\mu$m. In Fig. S6, we exhibit four additional AFM images of thick samples in the dry state, which thickness increases from left to right. We observe four volcano patterns with increasing wavelength and amplitude.

S3. QUANTITATIVE CHARACTERIZATION OF THE SAMPLES

A. Dry and wet PNIPAM film stiffnesses

Force spectroscopy measurements were performed using AFM on both dried and wet films to extract their

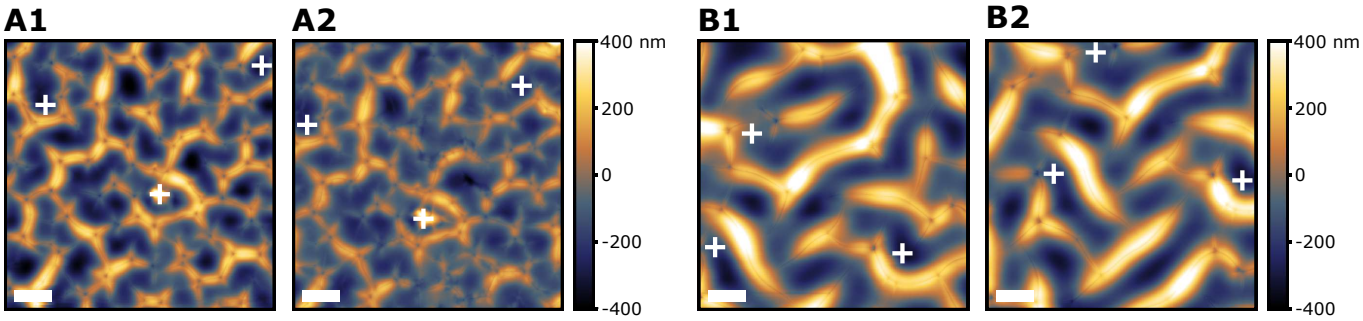

C

Concentration [w/w]	Spin-coating	Solvent	Drying	Result	Images
5%	3000 rpm	Acetone	RT conditions	Exact same pattern	
5%	3000 rpm	Acetone	N_2 drying	Same pattern type	
10%	1000 rpm	Acetone	RT conditions	Exact same pattern	B1 - B2
20%	1000 rpm	Acetone	N_2 drying	Exact same pattern; amplitude decrease	
10%	3000 rpm	Water	RT conditions	Exact same pattern	
10%	3000 rpm	Water	N_2 drying	Exact same pattern; amplitude decrease	A1 - A2
2%	3000 rpm	Water	RT conditions	Same pattern type	
2%	3000 rpm	Water	N_2 drying	Exact same pattern	

FIG. S4: **Comparison of surface topography before and after a swelling/drying cycle in different solvents.** *A) Topography measurement of a dry PNIPAM film, before (A1) and after (A2) immersion into water and drying. B) Same, in acetone. The films were prepared using experimental parameters indicated in panel C. The white bar represents* 15 μm. *The three white crosses are placed on remarkable spots to guide the eye in the comparison. C) Table of immersion experiments and observations. The images showed in panels A and B correspond to two samples, as indicated in the right column.*

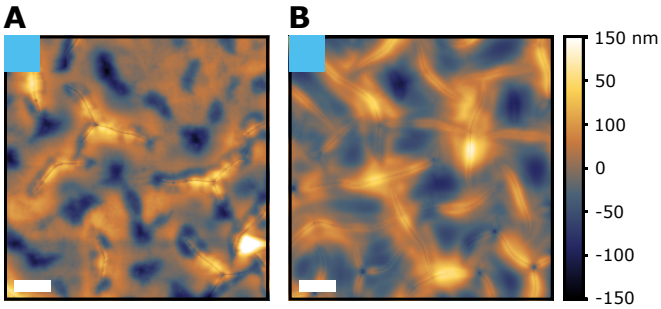

FIG. S5: **Comparison of two similar samples with different drying times.** *AFM images of two samples prepared in the exact same conditions, with initial dry thickness* $h = 2.02\,\mu$m, *and different rinsing times. A)* 30 *min. B) A few days. The white bar represents* 5 μm.

Young's modulus, as represented in Fig. S7. Prior to the spectroscopy measurement, the deflection sensitivity was calibrated for each probe on a hard surface, and the spring constant was measured from thermal noise [**?**]. The AFM measurements on dry and wet films were performed respectively using a sharp and standard tip (*Nanosurf*, model *Dyn190Al*, nominal stiffness 48 N/m) in tapping mode, and using either a thin cone-shaped tip (*Nanosensors*, model *qp-BioAC-Cl*, nominal stiffness 0.06 N/m) or a thin pyramidal-shaped tip (*BudgetSensors*, model *Tap150GD-G*, nominal stiffness 5.0 N/m), adjusting the stiffness effectively measured. The indentation range was kept small compared to the sample thickness and the drive approach velocity was slow to minimize the influence of Stokes drag. The AFM data were treated using the *AtomicJ* software [**?**], based on JKR model, taking into account the probe geometry and the finite thickness of the samples. In Figs. S7A and B we show respectively a typical AFM image of a patterned dried PNIPAM film and the measured Young's modulus as a function of the position of the measurement. On Fig. S7C, we show a histogram of the measured values of Young's modulus, we finally retain $E^{\mathrm{dry}} \approx 700 \pm 100$ MPa to be the Young's modulus of dried PNIPAM films. In Fig. S7D we show an AFM image of the same sample as in Fig. S7A but in the swollen state, which exhibits a creased pattern. In fig. S7E we show the measurement of the Young's modulus as a function of the position. Interestingly, the pattern shown on the AFM image can be guessed on the Young's modulus map. Unlike for dried films, we observe that the Young's modulus varies with the topography: the swollen gel is softer on the top of the bumps than in the depth of the dips. The latter observation may be due to an inhomogeneity of solvent fraction at the surface due to the crease-induced expulsion of solvent, and is consistent with a higher strain close to the creases [**?**]. Lastly, in Fig. S7F we show the histogram of the measured values of Young's modulus. We finally retain $E^{\mathrm{wet}} \approx 35 \pm 5$ MPa as the Young's modulus of swollen PNIPAM gels.

In order to check the dependency of the Young's mod-

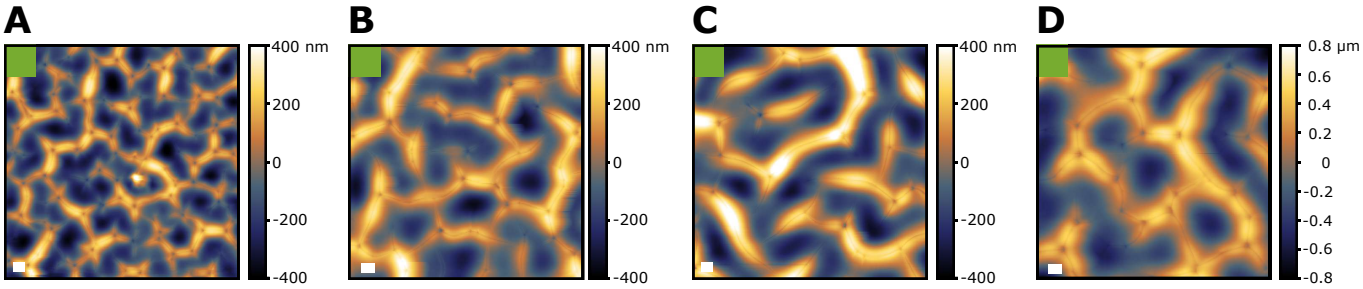

FIG. S6: **Volcano patterns.** *AFM images of thick samples, with initial dry thickness such that* $h > l_{\mathrm{ec}}^{\mathrm{wet}}/S_{\mathrm{R}}$*, with increasing thicknesses from left to right. A)* $h = 1.80\,\mu$m*. B)* $h = 2.69\,\mu$m*. C)* $h = 2.95\,\mu$m*. D)* $h = 4.55\,\mu$m*. The white bar represents* $5\,\mu$m*.*

ulus on the thickness, we also investigated thicker and thinner samples, with and without a pattern, and we show in Fig. S7G-L the measurements realized on two thinner ones. In Fig. S7G and H, we respectively show an AFM image of a swollen PNIPAM film that exhibitq a brain pattern when dry, and the measured Young's modulus in wet conditions as a function of the position of the measurement. On Fig. S7I, we show a histogram

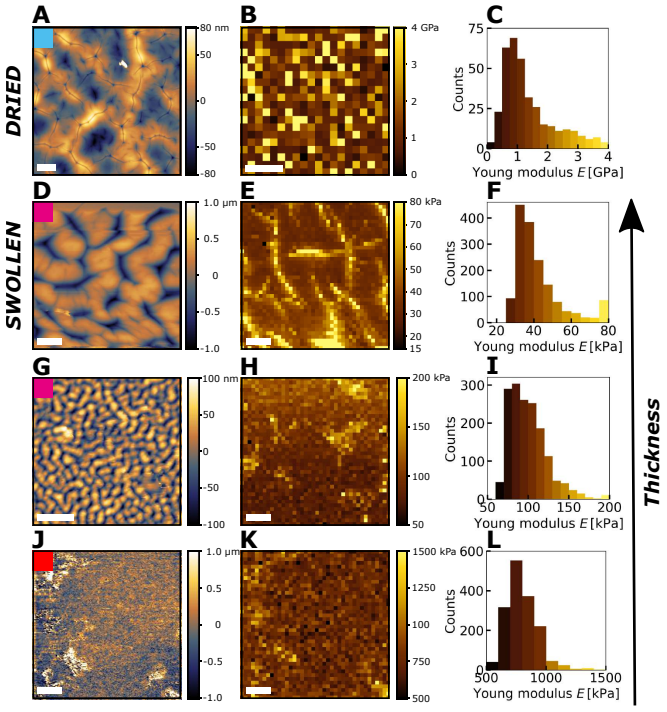

FIG. S7: **Measurement of the Young's modulus of PNIPAM films** *Left: AFM images of the investigated region. Middle: Measured Young's modulus E as a function of the position of the measurement. Right: histograms of the measured values of Young's modulus. A-C) For a PNIPAM film of dry thickness* $h = 950\,$nm*, in the dry state. D-F) For the same film as in A-C), but in the swollen state. G-I) For a film of dry thickness* $h = 320\,$nm *in the swollen state. J-L) For a film of dry thickness* $h = 25\,$nm*. The white bar represents* $5\,\mu$m*.*

of the measured values of Young's modulus. We measure a higher value as compared to the previous film, $E^{\mathrm{wet}} \approx 80 \pm 10\,$MPa but on the same order. Finally, in Figs. S7J,K and L we show the same as in Figs. S7G, H and I, but for an ultra-thin sample without a pattern. As opposed to the previous cases, we measure an increase of the Young's modulus by a factor 20. This observation is rationalized by recalling that the ultra-thin samples swell less, which is also why they exhibit no patterns. This may be a result of an increased crosslinking density close to the substrate, which does not have a higher density of functional groups than the polymers [**?** **?**]. For ultra-thin samples, swelling in insufficient to reach the critical threshold in strain associated in the unstable regime. As a result of this lesser swelling, the solvent concentration in the formed hydrogel is lower than in the case of thicker samples. Recalling that the Young's modulus varies with the solvent concentration [**?**] and that below a given solvent fraction the polymer films turns glassy [**?**], we thus expect to measure a significantly higher Young's modulus in ultra-thin samples.

In summary, we have verified that the measured Young's modulus is independent on the pattern, having cross-checked on brain-like and volcano samples. However, for ultra-thin sample, we do observe a significant increase of the Young's modulus, demonstrating that the smaller solvent volume fraction rends closer to the glass transition.

B. Precision of the estimation of the dry elastocapillary length

Based on observations, the wavelength of surface patterns in the swollen state λ^{wet} is expected to follow a period-doubling hypothesis:

$$\lambda^{\mathrm{wet}} = \begin{cases} 2\lambda & \text{for} \quad h \leq l_{\mathrm{ec}}^{\mathrm{wet}}/S_R, \\ \lambda & \text{for} \quad h \geq l_{\mathrm{ec}}^{\mathrm{wet}}/S_R, \end{cases} \tag{S1}$$

with λ the wavelength in the dry state, and $l_{\mathrm{ec}}^{\mathrm{wet}}/S_R$ the observed thickness transition between brain–like and volcano patterns. With this assumption, the wavelength in the wet state as a function of the thickness is fitted with

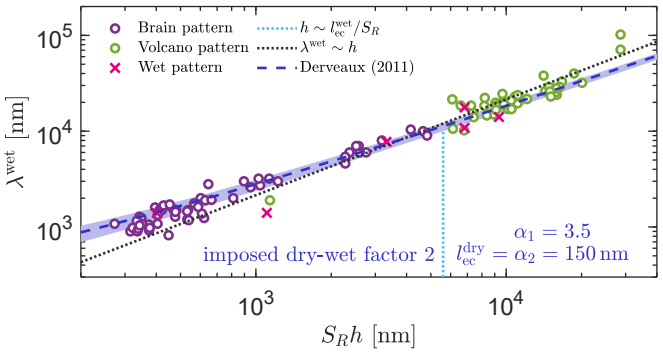

FIG. S8: **Estimation of the dry elastocapillary length** *Wavelength in the wet state* λ^{wet} *as a function of the wet thickness* $S_R h$*, using the period-doubling hypothesis as formulated in Eq.* (S1)*. The dark blue dashed line represents the fitted curve based on Eq.* (S2) *[?]. The shaded zone accounts for a* $\pm 50\,\%$ *of the fitting parameter* α_2*, that gives an estimate of the dry elastocapillary length.*

Dervaux and Ben Amar's model, as:

$$\lambda^{wet} = \alpha_1 4\pi h / \ln(44.953 h/\alpha_2), \qquad \text{(S2)}$$

with α_1 and α_2 being two fitting parameters, as represented on Fig. S8. In particular, α_2 gives a lengthscale, that estimates the elastocapillary length computed in the initial dry state, l_{ec}^{dry}. We obtain a prefactor of $\alpha_1 = 3.46$ and a dry elastocapillary length of $l_{ec}^{dry} \approx \alpha_2 = 150\,nm$. To indicate the precision of the estimated lengthscale in the dry state, the shaded area in Fig. S8 indicates how the fitted curve would be affected by a change in the interval $l_{ec}^{dry} \pm 50\,\%$. Indeed, the non-linear fit on Dervaux and Ben Amar's model does not provide a precise value, but an estimate for the dry elastocapillary length, and thus for a dry shear modulus of $G^{dry} \approx 280\,kPa$. The latter shear modulus would correspond that of the dry polymer films and would seem perfectly reasonable for a dry polymer film, if the PNIPAM did not undergo a glass transition upon drying. However, the estimate of l_{ec}^{dry} is reasonable enough to validate the use of Dervaux and Ben Amar's thickness-wavelength relation to explain our experimental data. As a conclusion, creases are formed at the free surface in the wet state with a prescribed spacing, which scales with the thickness albeit a logarithmic correction.